Nuclear Science and Techniques (2026) 37:52
https://doi.org/10.1007/s41365-025-01870-6

KONUS dynamics for a 750 MHz IH-based injector

J. Giner Navarro[1,4] · C. Oliver[1] · D. Gavela[1] · V. Bencini[2] · A. Lombardi[2] · P. Calvo[1] · G. Moreno[1] · M. León[1] · A. Rodríguez[1] · J. M. Carmona[3]

Received: 16 January 2025 / Revised: 28 March 2025 / Accepted: 7 May 2025 / Published online: 14 January 2026

Abstract
In response to the increasing demand for hadron therapy facilities, significant efforts have been directed toward enhancing the performance of high-gradient and high-transmission injectors for light ion beams. For carbon ion irradiations, which offer greater radiobiological efficiency in tumor treatment, recent research has focused on developing high-production sources of fully stripped C^{6+} ions and highly compact, high-frequency RFQ cavities. This study explores the design possibilities of a carbon ion acceleration section using 750 MHz Interdigital H-mode Drift Tube Linacs (IH-DTLs) as a high-efficiency solution for accelerating ions in the 5–10 MeV per nucleon energy range. A particle-tracking routine based on the TRAVEL code was developed to design the acceleration line through a tailored KONUS-type configuration. Three design solutions were proposed and compared, exploring different alternatives regarding the use of a MEBT to match the output beam phase space of the RFQ to the optics of the line, as well as varying considerations for magnetic systems to focus the beam. Additionally, the compatibility of the proposed solutions with the existing design of the carbon ion bent-linac for hadron therapy was assessed.

Keywords Accelerator · Injector · Linac · IH · KONUS dynamics · Hadron therapy

1 Introduction

Beam injectors in particle accelerators aim to provide an appropriate current intensity, determined by the intended application. Conventional hadron therapy facilities based on cyclotrons and synchrotrons are capable of operating in CW mode, as well as in short pulses to provide high-intensity beams. Given that cyclotrons are fixed-energy systems, absorbers are employed to shape the dose in the volume occupied by the tumor within the desired energy range. This is not the case for pulsed, all-linac systems under development [1, 2], which would allow for active and precise energy scanning of the beam and require sufficient charge input from the injector.

Compared to proton therapy beams, carbon ions are considered to exhibit well-balanced and optimal properties in terms of both physical and biologically effective dose localization in the body. This is due to the fact that carbon ion beams offer better dose distribution, concentrating sufficient dosage within target volumes while minimizing exposure to surrounding normal tissues [3, 4]. Accelerator facilities typically deliver relatively low currents on the order of 0.2 nA [5]. Higher amounts of ions within shorter pulses will

Project co-funded by European Union in the context of the pre-commercial public procurement of RD services managed by CDTI E.P.E. In particular, this work was developed and co-funded by the European Regional Development Fund (ERDF) as part of the project for the development of a Compact Linear Accelerator for Hadrontherapy, Exp. CPP 03/2023 AB (DCCPI/OCPI).

✉ J. Giner Navarro
jorge.giner@uv.es

✉ G. Moreno
Gabriela.Moreno@ciemat.es

[1] Department of Technology, CIEMAT, Avenida Complutense 40, 28040 Madrid, Spain

[2] Beams Department, CERN, 1211 Geneva, Switzerland

[3] Added Value Industrial Engineering Solutions, Xixilion Kalea 2, 20870 Elgoibar, Spain

[4] Instituto de Ciencia de los Materiales, Universitat de València, C/ Catedrático José Beltrán 2, 46980 Paterna, Spain

be required in emerging FLASH radiotherapy techniques [6, 7], which promise greater cell survival probability in healthy tissues surrounding the tumor [8].

The current provided by modern sources of fully stripped carbon ions, C^{6+}, is still limited. With their maximum available charge, the acceleration in linear injectors achieves greater efficiency owing to their higher charge-to-mass ratio, thereby offering greater compactness in length. Conventional hadron therapy injectors use C^{4+} sources, which must pass through a stripper and experience beam quality degradation [9].

These considerations highlight the importance of producing a sufficient amount of current in the initial stage of an accelerator. However, it is equally important to ensure proper beam transmission throughout all the components of a linear accelerator, and for this, effective diagnostic systems are necessary. This study explores the design possibilities of ion beam dynamics in a linear acceleration section composed of 750 MHz IH-DTL cavities, which could serve either for injection into a synchrotron or as one of the early low-beta acceleration stages of a linac. In particular, this study takes as a reference point the "bent-linac" conceptual design of the beam dynamics from CERN [10], which proposes a solution for a linear accelerator, folded in two halves and connected by a 180-degree bending, to minimize its footprint in a hospital environment. In this context, Quasi-Alvarez DTL-type structures have already been proposed [11] for the initial acceleration stages, as with a FODO-type configuration, they offer the advantage of preserving the alternating focusing dynamics of the beam originating from the RFQ. Nonetheless, IH cavities are known to be much more efficient as the proposed 750 MHz system achieves shunt impedances (effective ZT^2) exceeding 200 MΩ/m [12–14].

Here, we propose replacing the 5–10 MeV/u segment of the bent-linac modeled at CERN with an IH-DTL section. This entails adapting the expected alternating gradient lattice to one compatible with IH-type transverse dynamics and assessing the acceptance of the subsequent 3 GHz side-coupled drift tube linac (SCDTL) structures [15]. Given the low current transmission offered by the novel 750 MHz compact RFQ [16], achieving complete transmission in the following stages while maintaining a moderate beam emittance is of particular importance. In addition to assessing the need for a medium-energy beam transport (MEBT) at the RFQ exit, the tracking simulations conducted in this study allowed us to define the cavity specifications based on the behavior of longitudinal beam dynamics in a KONUS-type configuration. This design aims to provide maximum current transmission, with optimal acceleration efficiency.

Despite focusing here on a particular linac, the ultimate goal of this article is to highlight the potential for high compactness and efficiency of high-frequency IH-DTL cavities within an energy range of interest for future ion linacs, even beyond their applications in hadron therapy. The conceptual design of the bent-linac serves here as a specific context for designing the dynamics of this type of high-frequency structure, motivated by recent progress in the design and fabrication feasibility of 750 MHz IH-DTLs.

The remainder of this article is structured as follows. First, in Sect. 2, we review the state of the art of existing IH cavities and their various configurations. In Sect. 3, we present the reference beam properties and the code developed specifically to explore various options for beam dynamics, as well as the considerations raised in the specifications of the beamline elements. The results of the obtained solutions are detailed in Sect. 4, and conclusions are drawn in Sect. 5.

2 State of the art

The state of the art in IH-DTL cavity configurations is divided into two approaches to beam dynamics, aiming to ensure both transverse and longitudinal beam stability throughout its trajectory. One is the "combined zero-degree synchronous particle structure" (KONUS) [17] developed by GSI, for which functional designs have been implemented in medical facilities operating at 217 MHz [18]. This method sequences the acceleration and confinement processes into three stages. In the primary stage, the beam is accelerated along a section designed for a particle in a zero-degree synchronous phase to utilize the maximum electrical energy during acceleration. Although this synchronous phase does not provide stability, the strategy involves injecting the beam at a slightly higher energy than the synchronous particle and having the bunch describe only a portion of the phase space orbit around it before it is lost or blown up. The next stage is solely dedicated to beam focusing using magnets, either through solenoids or combinations of quadrupole triplets. These allow the beam to be reinjected into new gaps in the Drift Tube Linac of the third stage, responsible for rebunching the beam longitudinally to a typical synchronous phase of approximately −35°, while also providing some acceleration. With only a few gaps, it is sufficient to restart the three stages sequence of primary acceleration, refocusing, and rebunching.

The alternative strategy to KONUS is known as "alternating phase focusing" (APF), which avoids the use of magnets and makes use of the RF forces within the cavity itself to control confinement in both transverse and longitudinal directions. Under negative synchronous phase conditions, the bunch is longitudinally stable but defocused transversely. Conversely, positive-phase conditions result in debunching but provide transverse focusing. APF designs adjust the distances between gaps to stably alternate between these conditions in all three dimensions of the beam. The HIMAC carbon therapy facility adopted this configuration in an initial

200 MHz IH-DTL prototype [19], which was also adopted by other clinical centers in Japan [20]. A detailed comparison between KONUS and APF [21] revealed that the latter exhibited greater beam emittance growth owing to the nonlinear nature of the RF forces. It is also relevant to mention that the radial component of these focusing forces rapidly decreases with the beam energy, at a rate of γ^{-3}, where γ is the Lorentz relativistic factor [22]. Therefore, it is not advisable to adopt this configuration in the higher-energy sections of the injector.

In any case, certain manipulations of the phase at which the bunches are accelerated along the linac can be advantageous. Recently, a variation of the KONUS configuration was proposed [23, 24] in a 325 MHz IH structure integrated into a proton therapy synchrotron injector. On the one hand, the rebunching section was strengthened to a lower phase of −80°, to eliminate the need for bunchers in the MEBT. However, a number of debunching gaps at 10° were added at the end to provide transverse focusing and save on the use of magnets. This illustrates that while both strategies are extremely useful in ion injectors used in hadron therapy accelerators, there is some flexibility in their design for application in specific systems.

3 Methods

3.1 The code and the input beam

The beam dynamics designs presented in this study were conducted using TRAVEL [25], a simulation code for tracking charged particles through accelerator components, including quadrupole magnets and radiofrequency structures. An important feature of this code is its ability to introduce multiple gaps within a single RF unit with varying voltages and separation distances, considering the phase at which each individual particle accelerates in each gap. This allows for easy modeling of multi-cell cavities in any operating mode; in our case, for an IH-DTL structure in π mode for low-velocity ions.

The new beam dynamics designs proposed in this study are configured based on the output beam from the second RFQ of the bent-linac injector [10, 16]. At an output energy of 5 MeV per nucleon, the expected total charge of C^{6+} ions per pulse is up to 0.5 nC (or 5×10^8 ions), according to the nominal specifications. We have a distribution sample of 4218 macroparticles in the six-dimensional phase space in TRAVEL code format to configure the accelerator section design with IH cavities. The 2D projections of the beam distribution are shown in Fig. 1, and their statistical parameters are listed in Table 1. This corresponds to a nearly round beam that has been confined through the RFQ within an average radial aperture of only 1.4 mm. However, owing to the alternating quadrupolar structure of the RFQ, the beam occupies ellipses with opposite orientations for each transverse phase space plane, resulting in horizontal defocusing and vertical focusing behaviors. In the longitudinal plane, short bunches of the order of picoseconds were extracted, equivalent to 2.3 degrees of the rms phase with respect to the radiofrequency.

We developed a MATLAB script, assisted by TRAVEL, for the design of an acceleration line composed of IH cavities in the KONUS configuration. A series of parameters were defined for each of the three stages of a KONUS unit. In the zero-degree acceleration stage, we specify the number of gaps N_0, their effective acceleration voltages $\{V_i\}_{i=1}^{N_0}$ (including the transit-time factor across the cell), and the energy difference ΔW_0 and phase difference $\Delta\varphi_0$ of the asynchronous bunch at the entrance with respect to a fictitious synchronous particle. In the following stage, the characteristics of the magnets were defined. The script allows flexibility in the choice of magnet type; however, it is convenient to use a symmetric triplet system of quadrupoles, for which the gradients, magnetic lengths, and spacing between components must be specified. Finally, for the KONUS rebunching section, the required number of gaps N_r, their effective voltages $\{v_i\}_{i=1}^{N_r}$, and the synchronous phases $\{\varphi_i\}_{i=1}^{N_r}$ in each gap must also be defined. Some parameters were chosen a priori for convenience, such as the number of cells required for each section; however, the rest were determined using custom optimization algorithms based on Nelder–Mead routines. A previous exploration of the best starting KONUS parameters helped the optimizer find suitable solutions.

The design follows a beam emittance growth moderation strategy. In particular, in the longitudinal projection, the emittance is highly sensitive to the beam conditions at the entrance of the zero-degree asynchronous section. Figure 2 shows some examples of how the excess energy of the asynchronous bunch, the initial phase, or even the orientation of the bunch ellipse in the phase space affects its propagation along the section. The number of gaps in this stage is limited such that the center of the bunch reaches the minimum phase deviation with respect to the synchronous particle. The choice of the phase of the first gap does not exhibit, in some cases, as much sensitivity to emittance and is attempted to be kept in the range of 0° to 10° to maximize the beam output energy. If present, the preceding rebunching stage also allows for the manipulation of the bunch conditions at the entrance of the asynchronous stage to enhance optimization capabilities, either through the number of gaps or the bunching phase.

Simultaneously, the code aims to ensure the proper transmission of the beam. To achieve this, the magnets within the beamline are optimized, considering the loss of macroparticles owing to interception at the boundaries of the vacuum

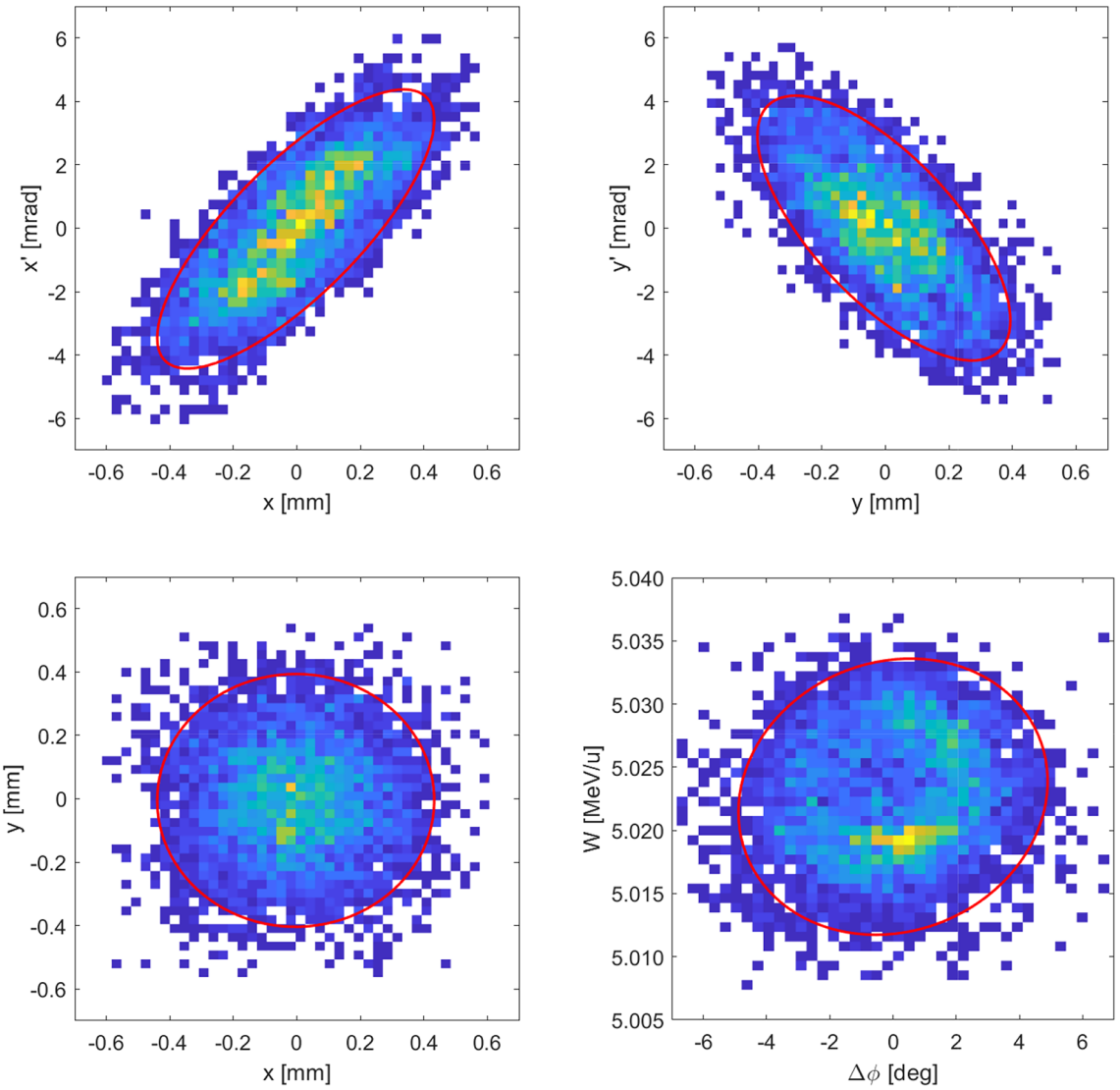

Fig. 1 (Color online) Projections of the transverse and longitudinal phase space of the beam at the RFQ exit. The solid red ellipse encloses 90% of the charge distribution

beampipe. For simplicity, the apertures of all components were defined with the diameter of a circular cross section, which is the most restrictive in the 5 mm bore of the IH drift tubes owing to power efficiency reasons. Regarding magnet optimization, the usual strategy involves fixing the length and position and exploring the optimal gradients. When optimizing a symmetric triplet of permanent magnet quadrupoles (PMQ), it is possible to set their lengths and the same gradient for all of them and optimize their positions to simplify, the fabrication of magnets as stacked modules of identical design. This optimization is fed back and forth into the beam simulations in the accelerating gaps, which also have a transverse defocusing effect.

Neither the effect of transverse electric fields on the beam orbit nor potential alignment errors are part of this study, which is why these features were not implemented in the code. In a previous study [26], the optimization of the drift tube geometry in the IH-DTL was addressed to minimize the effects of dipole kicks on the beam.

3.2 Magnet specifications and aperture considerations

The specifications of the magnets in the optimizer are subject to their manufacturability and the space they occupy along the line. Electromagnets offer flexibility in correcting potential beam errors. With normal-conducting resistive magnets, we consider a maximum magnetic field at the poles that is sufficiently below 1.5 T. The quadrupole gradients were then determined using the aperture of the poles. In the

Table 1 RMS values and Twiss parameters of the C^{6+} ion beam at the exit of the RFQ

Parameters	Values
σ_x (mm)	0.203
$\varepsilon_{x,\mathrm{norm\,rms}}$ (π mm·mrad)	0.0271
$\varepsilon_{x,\mathrm{norm\,90\%}}$ (π mm·mrad)	0.121
β_x (m/rad)	0.159
α_x	−1.25
σ_y (mm)	0.186
$\varepsilon_{y,\mathrm{norm\,rms}}$ (π mm·mrad)	0.0270
$\varepsilon_{y,\mathrm{norm\,90\%}}$ (π mm·mrad)	0.120
β_y (m/rad)	0.133
α_y	0.972
σ_z (deg)	2.28
	8.45 ps
	0.262 mm
$\Delta p/p$	5.1×10^{-4}
$\varepsilon_{z\,\mathrm{rms}}$ (π deg·MeV)	0.138
$\varepsilon_{z\,90\%}$ (π deg·MeV)	0.561
β_z (deg/MeV)	37.5
α_z	−0.112

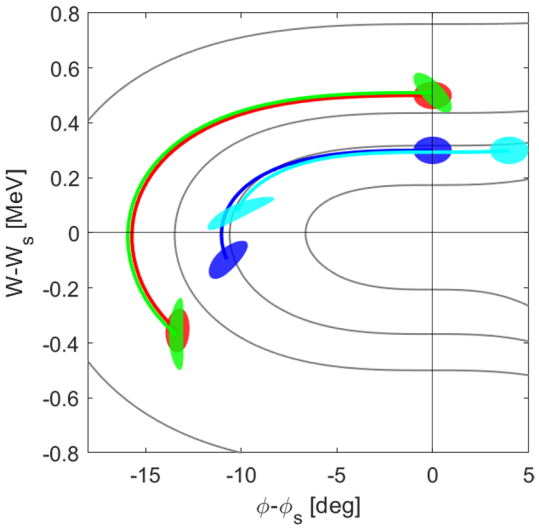

Fig. 2 (Color online) Four examples of the longitudinal phase space evolution (counterclockwise) across the zero-degree KONUS stage (50 gaps at 125 kV per gap, 750 MHz, π mode, and 60 MeV in energy of synchronous particle at the entrance)

designs of this study, the vacuum beampipes in the magnet sections were intended to have an inner diameter of 20 mm. Considering the thickness of the vacuum chamber and a small additional clearance, we adopted a maximum allowed pole radius of 13.5 mm, which corresponds to a maximum gradient of 110 T/m. When combined with other quadrupoles to form doublets or triplets, we also accounted for the separation between each singlet owing to their mechanical integration and the space occupied by the coil heads. In our current designs of resistive quadrupoles, a minimum separation of 75 mm is required, which is also sufficient to avoid fringe-field superposition.

However, we also consider the option of PMQs, which, although they do not allow user control of their focusing strengths, offer compact solutions without relying on electrical power consumption. These quadrupoles were designed in a conventional Hallbach configuration with 16 neodymium (NdFeB) blocks. This design eliminates the need for coil heads, allowing them to be joined to adjacent magnets without separation. The chosen material promises greater degradation resistance to radiation than other common magnets, such as samarium–cobalt (SmCo). The motivation for using PMQs lies in the possibility of integrating the KONUS focusing section within the RF cavity, with dedicated support and shielding design, as has been successfully tested in other setups [27–29]. In the proposed 750 MHz system, the compact size of the cavity at such a high frequency is the primary limitation for integrating the magnets; therefore, their mechanical design would pose a significant challenge, and manufacturing costs could increase. Initial calculations show the possibility of ensuring gradients of up to 88 T/m, with the same aperture as the resistive magnets, in systems that occupy only 75 mm in diameter, although very close to the expected profile size in the 750 MHz IH cavity [13]. The choice between PMQs and resistive magnets depends on a trade-off between complexity, manufacturing costs, compactness, and gradient-tuning capability. Neodymium magnets can slightly vary the magnetic field intensity by approximately 2%, through temperature control via a dedicated water cooling circuit. Integrating this circuit is even more challenging if the magnets are intended to be housed within the cavity; however, it remains a feasible option to consider if they are placed externally to correct minor beam dynamics errors.

3.3 RF voltage limitations

In the KONUS acceleration sections, we mentioned the requirement to define the effective voltages in the gaps. Higher voltages lead to higher beam energies in shorter segments. However, this is limited by the formation of vacuum breakdowns owing to excessively intense surface electric fields [30]. Electromagnetic simulations [12, 26] of single IH cells modeled in CST determined a confidence limit in the high-power performance of the RF cavity, which mainly depends on the gap size. The cell lengths of the IH cavities (near $\beta\lambda/2$ for π-mode structures) ranged from 20.6 to 29.1 mm in the acceleration range of 5 to 10 MeV per nucleon. The first cells have less space available for the acceleration gap, on the order of 8–9 mm, considering the size of the

stems and drift tubes that need to be machined. It is useful to consider that each IH tank, composed of a series of cells with increasing length, produces a uniform voltage profile; therefore, the cavity performance is determined by the maximum achievable level at the shortest cells.

In this study, we followed the same criterion of limiting the surface field to a maximum of 51 MV/m as used for the 750 MHz proton RFQ. Given the positive results during commissioning, this limit is considered high but safe under nominal conditions with 5 µs pulses and a repetition rate of up to 200 Hz. The maximum effective voltage per cell (including the transit-time factor) that can be reached at an energy of 5 MeV/u is 125 kV. Subsequent tanks with larger cell sizes and gaps allow for a higher voltage per cell, and the same surface field limitation criterion is applied based on the results of the electromagnetic simulation of individual cells.

We note that a uniform voltage profile across all cells is a first-order approximation of the profile that can be achieved after complete RF design of an IH tank. Therefore, it is necessary to iterate using the same code by introducing more realistic profiles and paying attention to the maximum surface field obtained from electromagnetic simulations.

4 Results and discussion

Hereafter, we outline a selection from a variety of solutions for the section with IH structures from 5 to 10 MeV/u following the KONUS configuration approach. We explored the option of using an initial MEBT to adapt the output beam optics from the RFQ to the interior of the IH cavities, considering the space requirements for other diagnostic systems.

4.1 Design proposal 1: without MEBT

First, we opted for the possibility of directly connecting the RFQ with the first IH tank, with a separation of only 10 cm to account for possible connections to the vacuum chamber. This entails carefully integrating the beam exiting the RFQ into the IH-DTL structure, which does not readily accept FODO-type optics, whereas other structures, such as the Quasi-Alvarez DTL [11] or SCDTL [15], offer a more suitable approach. The details of the transverse and longitudinal dynamics of this solution are shown in Fig. 3.

The strong defocusing of the beam in the horizontal plane allows for acceleration through only five drift tubes with a 5 mm aperture, requiring the immediate use of quadrupole magnets. In this case, the first five cells accelerated at a phase of −35°. At this point, the beam has also passed the beam waist, which exited the RFQ with vertical plane focusing. Therefore, we opted for a set of three PMQs of different lengths but with the same gradient, each with a 2 cm aperture, to reenter the following drift tubes. In this case, it is convenient to integrate the PMQs into the same cavity for two reasons. First, to avoid the manufacture of a separate IH cavity unit that is too short, as its end cells are potentially a source of electrical consumption [31]. However, as we have assessed later in this article, this may lead to the opposite effect if the tube containing the PMQs is excessively long, thereby carrying more RF currents. Second, this minimizes the space occupied by the magnets without controlling the longitudinal dynamics. We achieved a gap distance of 274 mm, equivalent to 13 times $\beta\lambda/2$ to meet the phase criterion within the same cavity. The remaining cells in the first IH tank are divided into a new rebunching section with 6 cells at −35° and an asynchronous zero-degree section with 35 cells. All gaps in this tank have an effective voltage of 125 kV, except for the cells at the ends and those adjacent to the body enclosing the PMQs, where a reduction of approximately half of the same voltage is expected. Following the first tank, a symmetrical triplet of PMQs was optimized to refocus the beam transversely and allow it to enter the second IH tank, which consists of four rebunching cells and 31 asynchronous acceleration cells at 145 kV per gap.

This solution is very compact, occupying approximately 3 m in length, and offers maximum transmission while maintaining moderate emittance throughout its phase space. At the exit of the second IH tank, a submillimeter (rms) round beam was obtained. In the longitudinal plane, the beam exited with a very short length of less than 1.5° (rms), although its energy spread almost doubled. We will see later that, for the beam to be adequately accepted in the 3 GHz SCDTL cavities, reducing its longitudinal length is more critical than the energy spread. The projections of the transverse and longitudinal phase spaces are shown in Sect. 4.5.

In practice, the initial cells of the first tank play the role of a pseudo-buncher, which cannot be operated independently, as they not only provide a certain amount of energy but also effectively preserve the longitudinal structure of the beam along the magnet section so that it can be accelerated later without affecting the emittance.

4.2 Design proposal 2: with MEBT, with buncher

Having an MEBT at the beginning of the section may be advisable to have greater control over the beam in the case of deviations from its nominal values. For this purpose, it is common to have quadrupoles to which steering correction magnets can be integrated to align and manipulate the beam transversely and thus ensure maximum transmission. Typically, these components should be associated with diagnostic systems that allow for proper correction adjustments. Similarly, a buncher is responsible for longitudinal plane control and allows limited control over the bunch length and energy spread at the entrance of the IH cavity.

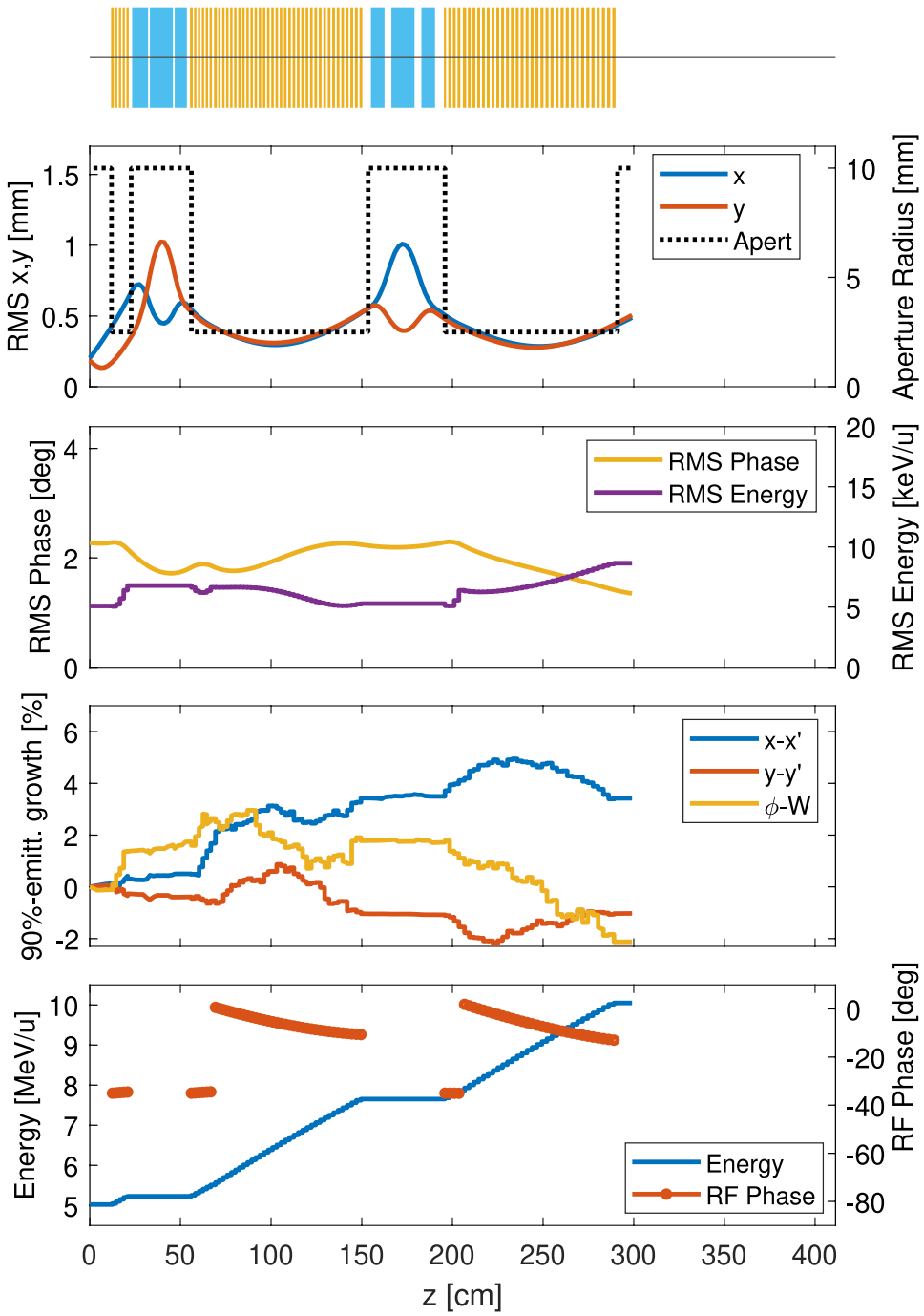

Fig. 3 (Color online) Beam dynamics of the solution without MEBT. On top, a beamline layout depicting quadrupole magnets in blue and RF gaps in yellow

In the design with MEBT design shown in Fig. 4, a three-gap buncher is used, each supplied with 90 kV and operating at −90°. The buncher is placed between three resistive quadrupoles that adapt the beam to focus on the first IH acceleration tank. Owing to the presence of the buncher, the first tank does not require a rebunching section following the KONUS method. Compared to the previous solution, this one divides the acceleration into three shorter tanks with 25 to 28 cells each, where the effective gap voltages are 125, 135, and 150 kV for the first, second, and last tanks, respectively. Between these three tanks, two series of symmetric PMQ triplets were optimized, although with opposite orientations to alternate the beam's focusing and defocusing effects.

In addition to the flexibility offered by this option, it achieves good transmission and preserves beam emittance. It also effectively controlled the energy dispersion at the exit of the third tank.

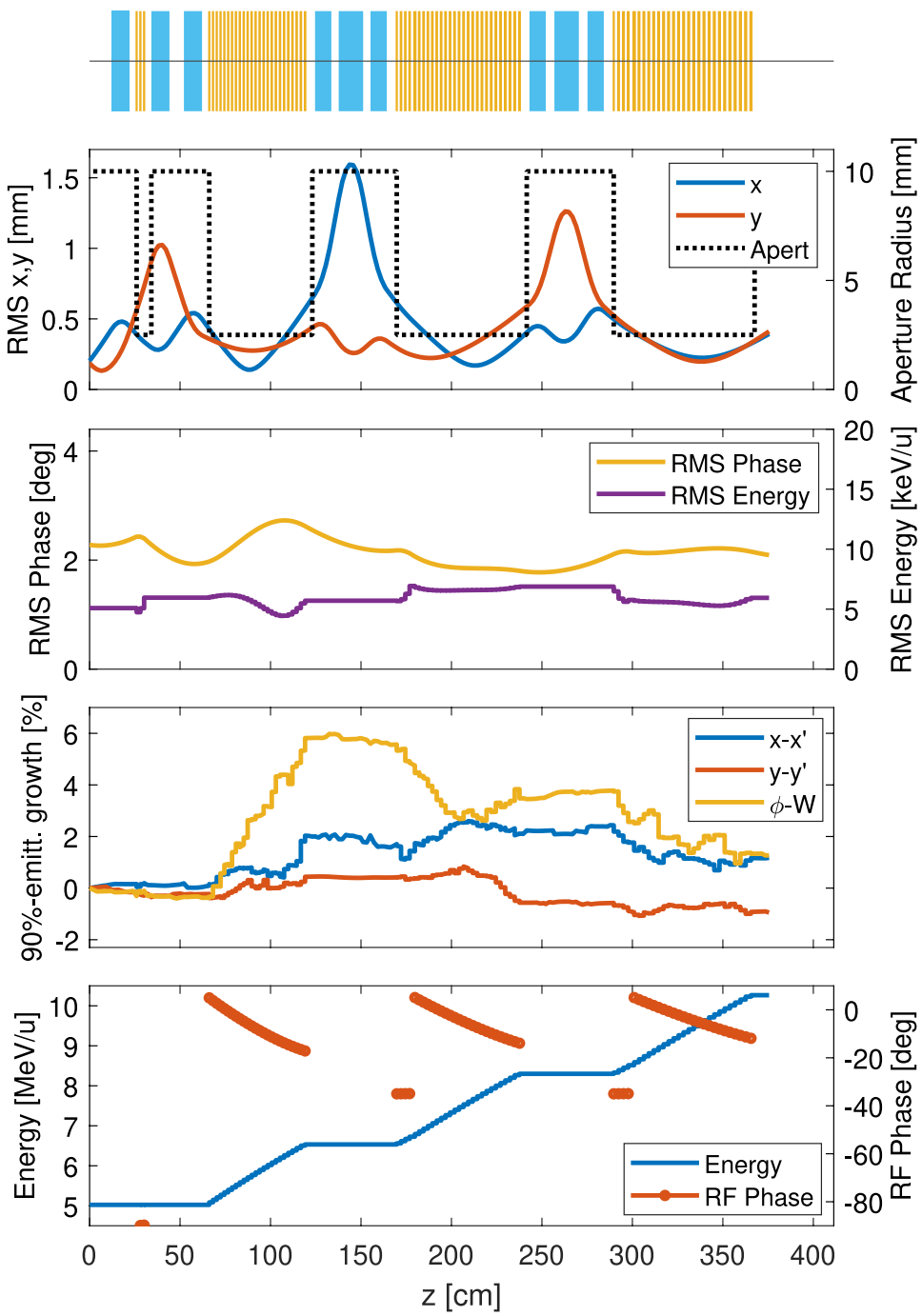

Fig. 4 (Color online) Beam dynamics of the solution with MEBT, with buncher. On top, a beamline layout depicting quadrupole magnets in blue and RF gaps in yellow

4.3 Design proposal 3: with MEBT, without buncher

In this proposal, we adopted an MEBT without a buncher, leaving sufficient space to accommodate a series of diagnostic systems and vacuum components that are considered minimally essential for the proper operation of the accelerator. A space of 40 cm is reserved at the beginning of the MEBT for a gate valve, an AC Current Transformer (ACCT) for current measurements, a Beam Position Monitor (BPM), and a Diagnostic Box (DBox) for beam size interceptive measurements [32]. This is followed by three resistive quadrupoles to adapt the beam optics to the IH tank acceptance.

The details of the dynamics are shown in Fig. 5. The MEBT occupies a total of 90 cm, which causes the bunch length to widen beyond 4° (rms) and presents problems for direct acceleration without affecting its emittance. Motivated by the modifications to the KONUS method in [24], we decided to use the first 10 gaps of the IH as an adapted rebunching section, starting at a phase of −90° (buncher mode) and linearly increasing to −35°. This allows for

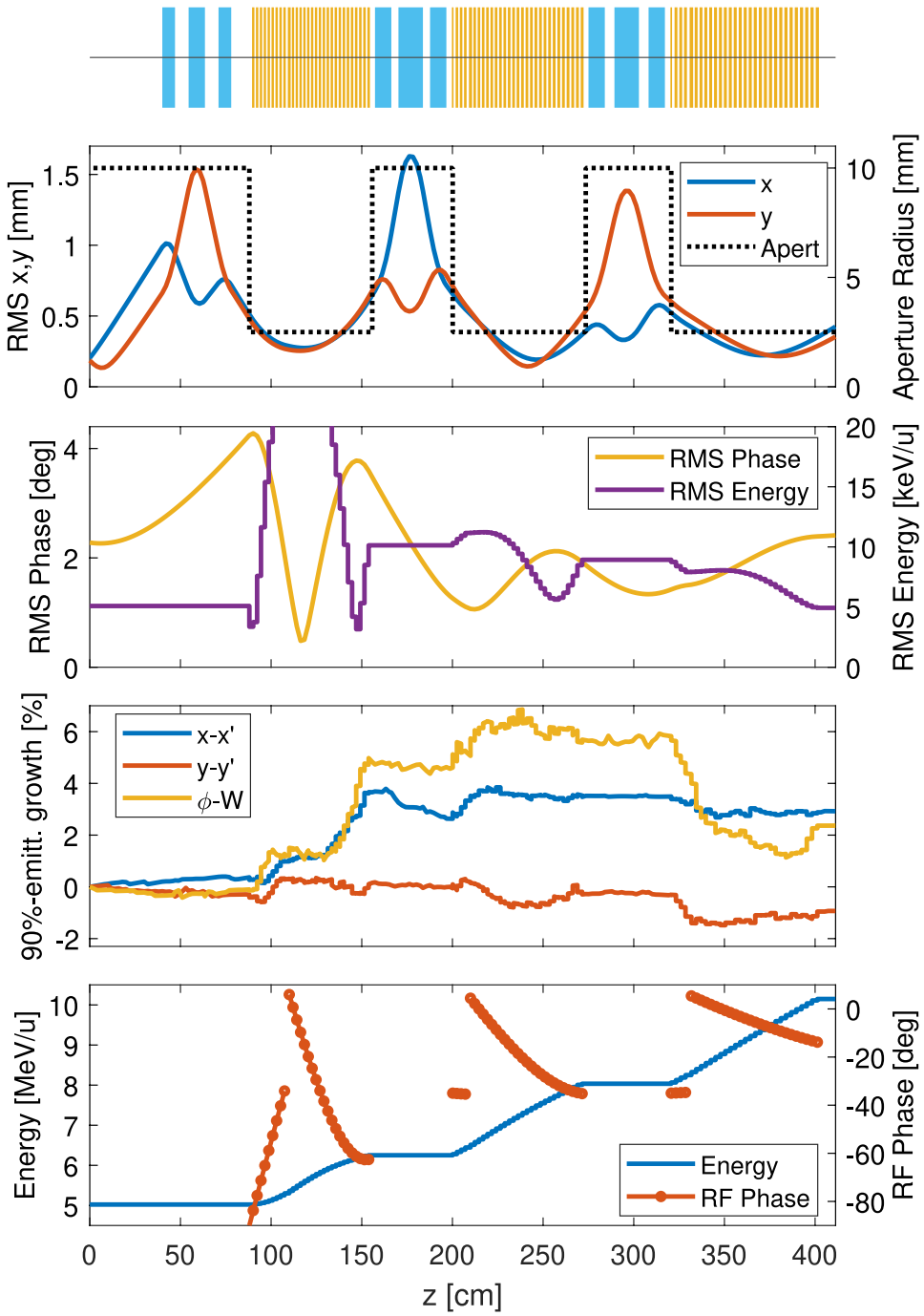

Fig. 5 (Color online) Beam dynamics of the solution with MEBT, without buncher. On top, a beamline layout depicting quadrupole magnets in blue and RF gaps in yellow

greater longitudinal acceptance of the beam without a significantly increase in the emittance. However, the bunch length quickly compresses, and its energy spread increases at the same rate. The remaining cavity cells follow an optimized asynchronous zero-degree section with a greater energy difference from the bunch than the synchronous particle. In this way, the energy spread was corrected to lower levels, and the bunch length was adjusted to reach a suitable value at the entrance of the second IH tank. The phase energy diagrams of the asynchronous sections of all three solutions are shown in Fig. 6.

With the configuration of the first tank, designed with effective gap voltages of 125 kV, the beam energy gain is reduced because it mostly operates at phases below −35°; however, it establishes better acceleration conditions for the subsequent tanks. The designs of the second and third tanks and PMQ triplets followed the standard

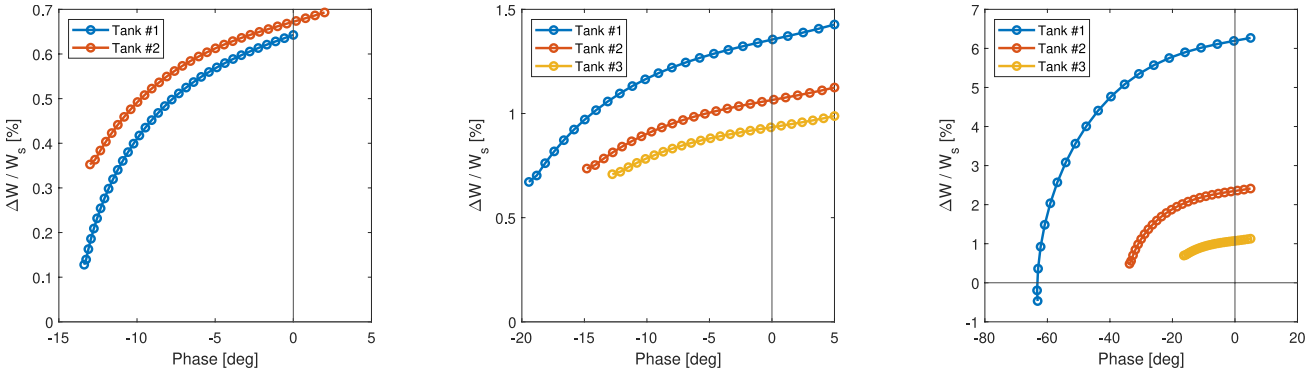

Fig. 6 (Color online) Phase energy diagram of the zero-degree asynchronous section of the IH tanks without MEBT (**a**), and with MEBT, with buncher (**b**) and without buncher (**c**). The surplus energy (in %) with respect to the synchronous particle energy is represented in the *y*-axis

optimization process, resulting in an output beam similar to that observed in the previous solutions.

4.4 Acceptance into 3 GHz SCDTL cavities of the bent-linac

To validate the integration of this new section into the designed bent-linac [10], a comparison was been made between the output beam and the acceptance of the rest of the beamline from 10 to 430 MeV/u. The new transition to 10 MeV/u involves a frequency jump from 750 MHz to 3 GHz, which occurred just after the RFQ in its original version. Additionally, the introduction of the new KONUS transverse optics requires adapting the beam back to a FODO-type lattice; therefore, it is essential to add a new transfer line for this purpose.

In this study, we considered the output beam of Design Proposal 3. The solutions from the other two proposals provided a very similar beam distribution, thus yielding analogous results. Figure 7 presents the comparison between this 10 MeV/u beam and the acceptance of the rest of the bent-linac up to 430 MeV/u in the three projections of the phase space. Using the TRAVEL code, a 68 cm long matching section was configured, consisting of three quadrupole electromagnets that matched the beam phase space to the transverse acceptance. The figure shows the correct orientation of the beam in the horizontal and vertical planes after matching the section. In the longitudinal plane, it can be observed that a wide energy spread is accepted, over 300 keV/u, but the bunch length becomes more critical due to the frequency jump, causing the bunch to occupy four times more space. Nevertheless, even though the bunch expands further along the matching section, over 95% of it fits within the acceptance area. For the beam distribution obtained in other proposals, such as Design Proposal 1, the matching transfer line would need to manage a wider energy spread beam but with a narrower bunch length. This was accomplished by attempting to limit the longitudinal emittance

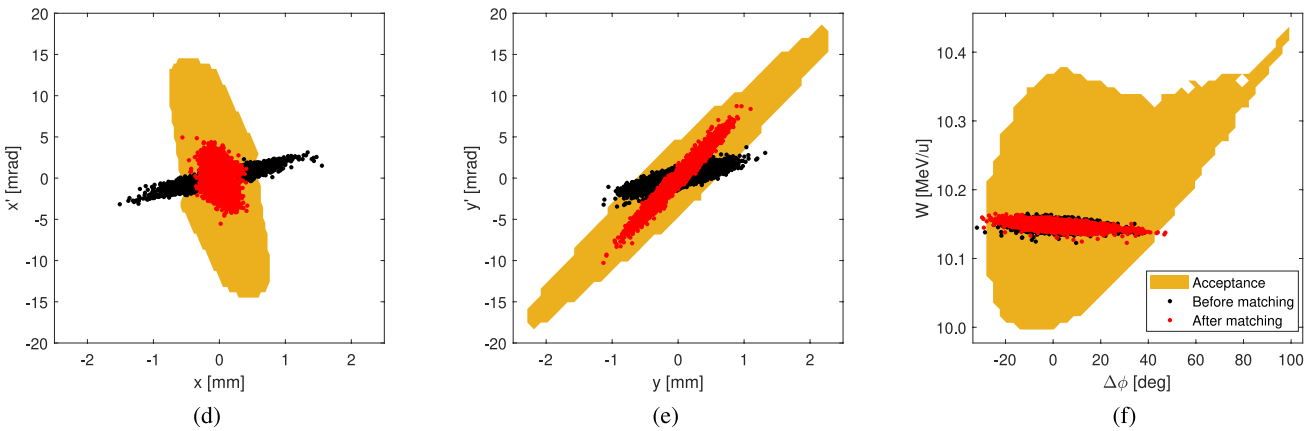

Fig. 7 (Color online) Projections of the beam phase in x-x' (**a**), y-y' (**b**) and the $\Delta\phi$-W at 3 GHz (**c**) at the exit of the IH cavities section and downstream the matching section, superpositioned to the acceptance area of the "bent-linac" optics from 10 to 430 MeV/u

growth in all proposals. An adequately matched transport line with a similar length produces the same bunch length entering the 3 GHz linac section and is still acceptable.

4.5 Comparison of design proposals

The three beam dynamics solutions are shown in Figs. 3, 4, and 5 using the same plot scales to visually enhance comparability. The phase space projections of the output beam in the transverse and longitudinal planes are shown in Fig. 8.

In Table 2, we summarize the most relevant design characteristics. These include the number of cells in each tank, voltage provided by each cell and total voltage across the entire structure, RF power losses generated by the IH cavities (buncher consumption has not been accounted for in Design Proposal 2), and length of the cavities and total space occupied by the full section, including the MEBT and focusing magnets. Finally, the table shows the results of emittance growth (defined by 90% of the beam) at the end of the line for each proposal, relative to the input beam emittance specified in Table 1. As we had set as the objective function of the code, in all design proposals, we demonstrated the ability to contain the emittance in all phase space planes to a value below 4%. Additionally, all proposals achieve nearly total transmission, with over 99.5% transmission, using the input beam sample distribution described in Sect. 3.1.

To assess power consumption, an estimation was conducted through electromagnetic simulations with CST of various individual cells across a wide range of lengths, as well as the end cells, as documented in [12, 13, 31]. Such estimation does not account for the arrangements necessary for assembling the cavity components and their auxiliaries but is calculated based on the simplest model. Therefore, the power values recorded in the table appear to be underestimated, although they are consistent across all cases, enabling an approximate comparison.

It is clear that incorporating an MEBT after the RFQ increase the space requirements for the entire section. The minimum extra space required is almost 80 cm, compared to the solution without MEBT, which includes a buncher but does not leave room for other diagnostics that are typically highly useful in beam operations. In the case of having some space for diagnostics, even without using a buncher, the MEBT consumes over one meter of space.

In Design Proposal 3, a higher voltage is required to accelerate particles to the same energy because lower initial phases are required for emittance growth moderation. As a result, the RF power consumption was approximately 24 kW higher than that in the case with a buncher. Considering the additional losses in the buncher itself, the overall RF consumption difference was smaller.

The scenario of Design Proposal 1, without an MEBT, represents the most compact solution; however, it is noteworthy that the power losses are somewhat higher than in the previous cases, despite utilizing only two tanks. The losses were primarily concentrated in the first tank, which incorporated a triplet of encapsulated PMQs in a larger drift tube. The dimensions of this anomalously long drift tube, which would require separating the two tank sections by 274 mm, would lead to a significant source of RF losses.

5 Summary and conclusions

This article proposes to take advantage of the high efficiency performance of H-mode cavities for a linear injector of carbon ion beams starting from 5 MeV/u and presents some alternatives to the baseline design of the CERN's bent-linac for a hadron therapy facility.

The detailed script presented here, based on the TRAVEL tracking code, has proved to be functional for beam dynamics design for IH cavities in the standard

Table 2 Summary of solutions for the IH cavity section in the 5–10 MeV/u range

Design proposal	Number of cells	Voltage		RF power		Length		90% emittance growth		
	Tank	Gap	Total	Tank	Total	Only tanks	Total	$\varepsilon_{x\,90\%}$	$\varepsilon_{y\,90\%}$	$\varepsilon_{z\,90\%}$
		(kV)	(MV)	(kW)	(kW)	(m)	(m)			
1.Without MEBT	46	125	10.4	156	250	1.95	2.99	+3.4%	−1.0%	−2.1%
	35	145		94						
2.With MEBT, with buncher	25	125	11.0	52	201[†]	2.03	3.76	+1.2%	−0.9%	+1.3%
	28	135		67						
	28	150		82						
3.With MEBT, without buncher	31	125	12.0	65	225	2.18	4.11	+2.9%	−0.9%	+2.4%
	30	135		72						
	30	150		88						

[†] Does not account for RF buncher consumption

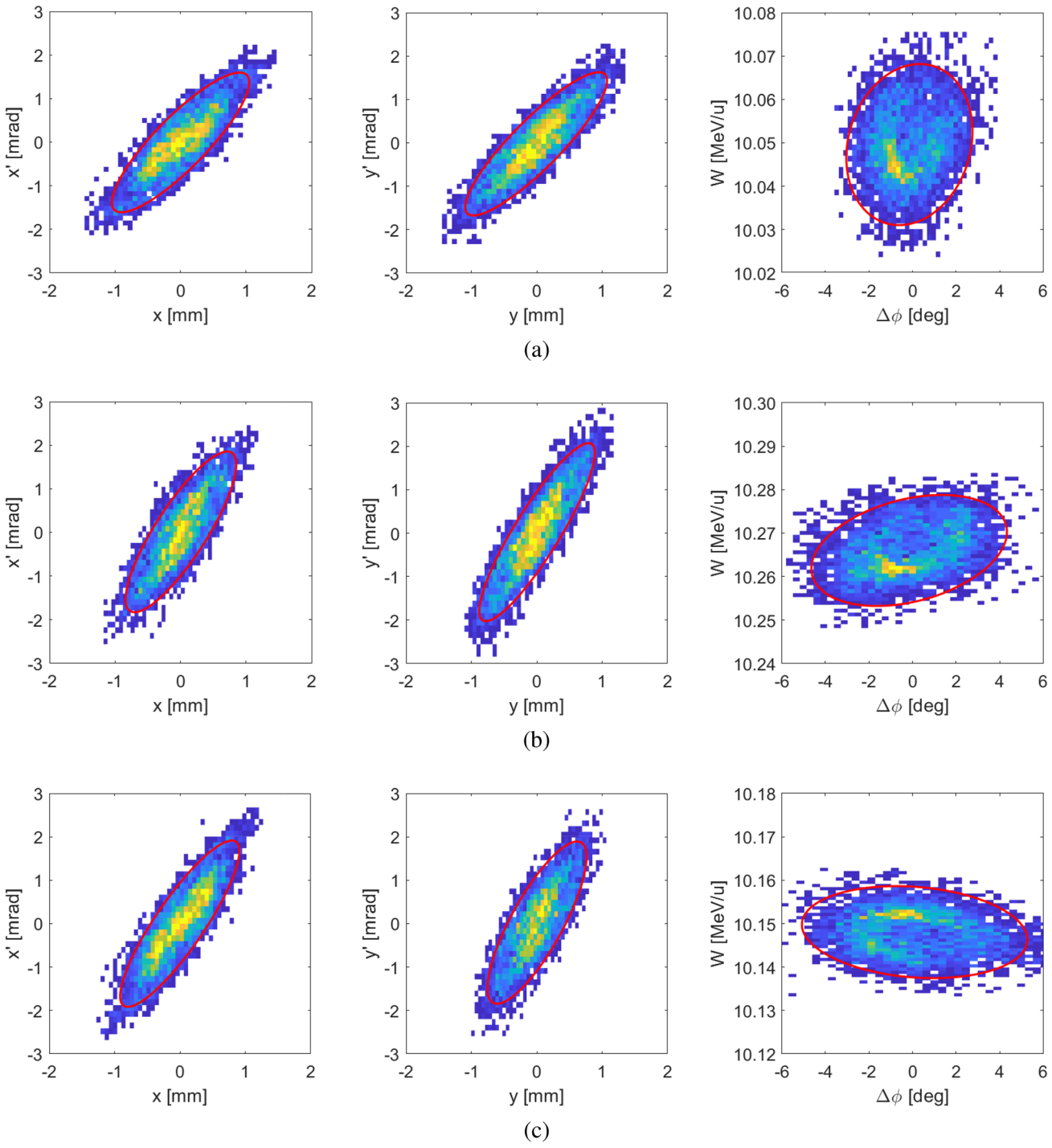

Fig. 8 (Color online) Projections of the transverse and longitudinal phase space of the beam at the exit of **a** Design Proposal 1, **b** Design Proposal 2, and **c** Design Proposal 3 of IH-DTL section. The solid red ellipse encloses 90% of the charge distribution

KONUS configuration, as well as in modified versions tailored to specific dynamic requirements. This is demonstrated by the three solutions proposed under very different conditions to achieve similar output beams: in the first, without an MEBT at the RFQ exit, and in the other two, with an MEBT that includes or excludes a buncher. The authors would like to clarify that none of the proposals deserves greater consideration than the others, as one of the objectives of this work is to exploit the capabilities of the beam dynamics and tracking code under the different conditions presented, which may be useful for the new design or upgrade of other linacs.

As a comparative analysis, the baseline design of the fixed-energy bent-linac, for the same energy range, occupies a length of 1.59 m [10], and we estimate a total power consumption of 1.7 MW, based on the orientative shunt impedances achieved by 3 GHz DTLs for these energies at their best performance [33]. Although IH cavities introduce a change in transverse optics and require more space than SCDTLs, these solutions provide greater power efficiency and are compatible with proper acceptance in the rest of the 3 GHz cavities at energies above 10 MeV/u.

An area that requires further study is the possibility of integrating encapsulated permanent magnets inside an IH tank, as proposed in Design Proposal 1, without the MEBT. This is the most compact solution that can be achieved without requiring a large MEBT, although we have noted significant efficiency degradation due to RF losses in an excessively long drift tube.

To improve compactness and efficiency, the challenge lies in manufacturing this type of structure at 750 MHz for the first time, compared to the current state-of-the-art RF frequencies of up to 325 MHz. The feasibility of these structures is being studied through electromagnetic and mechanical design analyses. The study presented here represents a necessary starting point for defining the specifications of the elements in this injector. Given that the collaboration remains interested in furthering its work on this topic, the technical and engineering complexities of manufacturing and commissioning will be addressed in the near future.

Author contributions All authors contributed to the study. The conception and design were led by J. Giner Navarro, C. Oliver, and D. Gavela. Material preparation and data analysis were carried out by J. Giner Navarro. In addition, V. Bencini and A. Lombardi were responsible for providing resources and supervision. The first draft of the manuscript was written by J. Giner Navarro, and all authors commented on previous versions of the manuscript. All authors read and approved the final version of the manuscript.

Funding Open Access funding provided thanks to the CRUE-CSIC agreement with Springer Nature.

Declarations

Conflict of interest The authors declare that they have no conflict of interest.

References

1. S. Verdú-Andrés, U. Amaldi, Á. Faus-Golfe, CABOTO, a high-gradient linac for hadrontherapy. J. Radiat. Res. **54**, i155–i161 (2013). https://doi.org/10.1093/jrr/rrt053
2. A. Degiovanni, G. De Michele, R. Bonomi et al., Design, integration, and commissioning of the first linac for image guided hadron therapy prototype. Phys. Rev. Accel. Beams **27**, 054701 (2024). https://doi.org/10.1103/PhysRevAccelBeams.27.054701
3. T. Kamada, H. Tsujii, H. Tsuji et al., Benefit of carbon ion radiotherapy in the treatment of radio-resistant tumors. AIP Conf. Proc. **680**, 1142–1145 (2003). https://doi.org/10.1063/1.1619910
4. H. Tsujii, T. Kamada, A review of update clinical results of carbon ion radiotherapy. Jpn. J. Clin. Oncol. **42**, 670–685 (2012). https://doi.org/10.1093/jjco/hys104
5. A. Degiovanni, U. Amaldi, Proton and carbon linacs for hadron therapy. in *27th International Linear Accelerator Conference*, p. FRIOB02 (2014)
6. U.A. Weber, E. Scifoni, M. Durante, FLASH radiotherapy with carbon ion beams. Med. Phys. **49**, 1974–1992 (2022). https://doi.org/10.1002/mp.15135
7. W. Tinganelli, U. Weber, A. Puspitasari et al., FLASH with carbon ions: tumor control, normal tissue sparing, and distal metastasis in a mouse osteosarcoma model. Radiother. Oncol. **175**, 185–190 (2022). https://doi.org/10.1016/j.radonc.2022.05.003
8. M.C. Vozenin, P. De Fornel, K. Petersson et al., The advantage of FLASH radiotherapy confirmed in mini-pig and cat-cancer patients. Clin. Cancer Res. Off. J. Am. Assoc. Cancer Res. **25**, 35–42 (2019). https://doi.org/10.1158/1078-0432.CCR-17-3375
9. S.Y. Lee, W.M. Tam, Z. Liu, Strip injection for carbon ion synchrotrons. Rev. Sci. Instrum. **78**, 096104 (2007). https://doi.org/10.1063/1.2786933
10. V. Bencini, Design of a novel linear accelerator for carbon ion therapy. Ph.D. thesis, Rome U., Rome (2020)
11. M.R. Khalvati, V. Bencini, S. Ramberger, Quasi-Alvarez drift-tube linac structures for heavy ion therapy accelerator facilities. Phys. Rev. Accel. Beams **26**, 022001 (2023). https://doi.org/10.1103/PhysRevAccelBeams.26.022001
12. J. Giner Navarro, G. Moreno, D. Gavela et al., Conceptual RF design of 750 MHz IH cavities for $\beta = 0.10 - 0.15$ ion beams in medical accelerators. Nucl. Eng. Technol. **56**, 3536–3544 (2024). https://doi.org/10.1016/j.net.2024.04.001
13. G. Moreno, M.C. Battaglia, P. Calvo et al., Effect of high-magnetic field region geometry on the efficiency of a 750 MHz IH structure. (JACOW Publishing, Geneva, Switzerland, 2022), pp. 150–153. https://doi.org/10.18429/JACoW-LINAC2022-MOPOGE05
14. S. Benedetti, High-gradient and high-efficiency linear accelerators for hadron therapy. Ph.D. thesis, EPFL, Lausanne (2018). https://doi.org/10.5075/epfl-thesis-8246
15. C. Ronsivalle, L. Picardi, A. Ampollini et al., First acceleration of a proton beam in a side coupled drift tube linac. Europhys. Lett. **111**, 14002 (2015). https://doi.org/10.1209/0295-5075/111/14002
16. V. Bencini, H.W. Pommerenke, A. Grudiev et al., 750 MHz radio frequency quadrupole with trapezoidal vanes for carbon ion therapy. Phys. Rev. Accel. Beams **23**, 122003 (2020). https://doi.org/10.1103/PhysRevAccelBeams.23.122003
17. U. Ratzinger, The IH-structure and its capability to accelerate high current beams. in *Conference Record of the 1991 IEEE Particle Accelerator Conference*. (IEEE, San Francisco, CA, USA, 1991), pp. 567–571. https://doi.org/10.1109/PAC.1991.164367
18. Y.R. Lu, S. Minaev, U. Ratzinger et al., The compact 20 MV IH-DTL for the Heidelberg Cancer Therapy Facility, in *Proceedings of LINAC 2004*. Lubeck, Germany, 2004

19. Y. Iwata, S. Yamada, T. Murakami et al., Alternating-phase-focused IH-DTL for an injector of heavy-ion medical accelerators. Nucl. Instrum. Methods Phys. Res. Sect. A **569**, 685–696 (2006). https://doi.org/10.1016/j.nima.2006.09.057
20. K. Yamamoto, H. Tanaka, H. Harada et al., Experimental verification of an APF linac for a proton therapy facility. Nucl. Instrum. Methods Phys. Res. Sect. B **269**, 2875–2878 (2011). https://doi.org/10.1016/j.nimb.2011.04.046
21. S. Minaev, U. Ratzinger, B. Schlitt, APF or KONUS drift tube structures for medical synchrotron injectors-a comparison. *Proceedings of the 1999 Particle Accelerator Conference (Cat. No.99CH36366)*. Vol. 5, pp. 3555–3557. (1999). https://doi.org/10.1109/PAC.1999.792368
22. Y. Lu, Development of an IH-DTL injector for the Heidelberg cancer therapy project, in *Ph.D. thesis*, Universitätsbibliothek Johann Christian Senckenberg (2005)
23. R. Tang, Q. Xing, S. Zheng et al., IH-DTL design with modified KONUS beam dynamics for a synchrotron-based proton therapy system. Nucl. Instrum. Methods Phys. Res., Sect. A **920**, 50–57 (2019). https://doi.org/10.1016/j.nima.2018.10.125
24. P. Ma, R. Tang, Y. Yang et al., Development of a compact 325 MHz proton interdigital H -mode drift tube linac with high shunt impedance. Phys. Rev. Accel. Beams **24**, 020101 (2021). https://doi.org/10.1103/PhysRevAccelBeams.24.020101
25. A. Perrin, J.F. Amand, T. Mütze, et al., TRAVEL v4.07 user manual. Internal Note, CERN (2017)
26. R. López López, M.C. Battaglia, P. Calvo et al., Cell geometry optimization for dipole kick correction in a high-frequency IH structure. (JACOW Publishing, Geneva, Switzerland, 2022), pp. 146–149. https://doi.org/10.18429/JACoW-LINAC2022-MOPOGE04
27. U. Ratzinger, Commissioning of the new GSI high current linac and HIF related RF linac aspects. Nucl. Instrum. Methods Phys. Res. Sect. A **464**, 636–645 (2001). https://doi.org/10.1016/S0168-9002(01)00155-3
28. H. Hähnel, U. Ratzinger, R. Tiede, The KONUS IH-DTL proposal for the GSI UNILAC poststripper linac replacement. J. Phys. Conf. Ser. **874**, 012047 (2017). https://doi.org/10.1088/1742-6596/874/1/012047
29. Y. Lee, E.S. Kim, Z. Li et al., IH-DTL design with KONUS beam dynamics for KHIMA project. Nucl. Instrum. Methods Phys. Res. Sect. A **801**, 51–57 (2015). https://doi.org/10.1016/j.nima.2015.07.048
30. W.D. Kilpatrick, Criterion for vacuum sparking designed to include both rf and dc. Rev. Sci. Instrum. **28**, 824–826 (1957). https://doi.org/10.1063/1.1715731
31. G. Moreno, J. Giner Navarro, D. Gavela et al., H11(0) end cells for a 750 MHz IH structure. IPAC'23 - 14th International Particle Accelerator Conference, (JACoW Publishing, Geneva, Switzerland, 2023), pp. 1681–1684. https://doi.org/10.18429/jacow-ipac2023-tupa171
32. M. Koopmans, D. Gavela, F. Di Lorenzo et al., Preparations for beam commissioning of the carbon RFQ at CERN. IPAC'23 - 14th International Particle Accelerator Conference, (JACoW Publishing, Geneva, Switzerland, Venice, Italy, 2023), pp. 4961–4964. https://doi.org/10.18429/jacow-ipac2023-thpm057
33. S. Benedetti, A. Grudiev, A. Latina, High gradient linac for proton therapy. Phys. Rev. Accel. Beams **20**, 040101 (2017). https://doi.org/10.1103/PhysRevAccelBeams.20.040101